fluids

MDPI

Article

Understanding the Application of Emulsion Systems for Bacterial Encapsulation and Temperature-Modulated Release

Nur Suaidah Mohd Isa [1,2,*], Hani El Kadri [1], Daniele Vigolo [1,3,4], Nur Farra Adlina Mohamed Zakhari [2] and Konstantinos Gkatzionis [1,5,*]

[1] School of Chemical Engineering, University of Birmingham, Birmingham B15 2TT, UK; dabigribosome@gmail.com (H.E.K.); daniele.vigolo@sydney.edu.au (D.V.)
[2] Faculty of Fisheries and Food Science, Universiti Malaysia Terengganu, Kuala Terengganu 21030, Malaysia; farra.adliina@gmail.com
[3] School of Biomedical Engineering, The University of Sydney, Sydney, NSW 2006, Australia
[4] The University of Sydney Nano Institute, The University of Sydney, Sydney, NSW 2006, Australia
[5] Department of Food Science and Nutrition, University of the Aegean, Metropolite Ioakeim 2, 81400 Myrina, Lemnos, Greece
* Correspondence: n.suaidah@umt.edu.my (N.S.M.I.); kgkatzionis@aegean.gr (K.G.)

Abstract: The encapsulation of bacteria in emulsion droplets offers various advantages over other conventional methods of encapsulation, such as improvements in bacterial viability, and may serve as microenvironments for bacterial growth. Nevertheless, changes in temperature may affect bacterial viability and droplet stability. In this study, the encapsulation of bacteria in single water-in-oil (W/O) and double water-in-oil-in-water ($W_1/O/W_2$) emulsions under cold storage and temperature-modulated release were investigated. The microencapsulation of bacteria in emulsion droplets was achieved by using a flow-focusing microfluidic device. Droplet stability was determined by measuring changes in droplet size and creaming behaviour at different temperatures. The thermal properties of the samples were determined by using differential scanning calorimetry, while the release of bacteria with changes in temperature was determined by measuring the colony form unit (CFU) of the released bacteria and conducting fluorescence microscopy. Higher bacterial viability was observed for encapsulated samples compared to free cells, indicating the ability of the emulsion system to improve bacterial viability during cold-temperature storage. The crystallisation temperature was lowered in the presence of bacteria, but the melting temperature was similar with or without bacteria. Storage in freezing temperatures of −20 °C and −80 °C led to extensive droplet destabilisation, with the immediate release of encapsulated bacteria upon thawing, where the temperature-modulated release of encapsulated bacteria was achieved. This study provides an overview of the potential application of emulsion droplets for bacterial encapsulation under cold-temperature storage and the controlled release of encapsulated bacteria mediated by changes in temperature, which is beneficial for various applications in industries such as food and pharmaceuticals.

Keywords: microfluidics; bacterial release; W/O/W emulsion; stability; crystallisation

Citation: Mohd Isa, N.S.; El Kadri, H.; Vigolo, D.; Mohamed Zakhari, N.F.A.; Gkatzionis, K. Understanding the Application of Emulsion Systems for Bacterial Encapsulation and Temperature-Modulated Release. *Fluids* **2024**, *9*, 274. https://doi.org/10.3390/fluids9120274

Academic Editors: Nilanjan Chakraborty, Maurizio Santini, Koji Hasegawa and Alireza Mohammad Karim

Received: 24 September 2024
Revised: 28 October 2024
Accepted: 30 October 2024
Published: 22 November 2024

1. Introduction

Emulsion droplets have been extensively studied to support the encapsulation of materials such as bacteria, bioactive compounds, and drugs [1–5]. These materials usually require storage at low temperatures to maintain their stability, especially for long-term storage. The storage of bacteria at low temperatures is a common practice for bacterial preservation to maintain their viability and is used for, for example, lactic acid bacteria in the dairy industry and in biotechnology applications. The freezing of cells to temperatures such as −20 °C and −80 °C helps to maintain not only their viability but also their functionality over a long storage period [6,7]. The encapsulation of bacteria in emulsions, especially food-based emulsions such as milk and ice cream, has been reported to improve bacterial

viability during freezing, depending on the nature of the emulsion [8–11]. Nevertheless, further studies are still required not only to assess the viability of bacteria encapsulated in emulsion droplets but also to determine the effect of bacteria on emulsion stability during storage at cold temperatures.

The successful application of emulsion droplets for bacterial encapsulation depends on their stability. The stability of emulsions during cold-temperature storage is highly affected by changes in the phase behaviour of the oil and aqueous phases, as reported in many related studies [12–15]. The crystallisation of the oil phase followed by the aqueous phase in oil-in-water (O/W) emulsions may cause a partial coalescence of the oil droplets whereby, in loosely packed emulsions, the collision between the still-liquid oil droplets and crystallised oil droplets with protruding crystals may cause membrane rupture, resulting in the droplets with still-liquid oil to flow out, forming a linkage between the two droplets as they freeze. This mechanism causes droplet flocculation, which eventually leads to complete coalescence and oiling-off upon thawing [12,16]. A different destabilisation mechanism for multiple emulsions, namely, water-in-oil-in-water ($W_1/O/W_2$) emulsions, has been proposed, which involves the external coalescence of the inner W_1 phase with the outer W_2 phase, which occurs during the thawing process, while the W_1 inner phase remains intact during the freezing process [17,18].

Although emulsion destabilisation is unfavourable for food emulsions as it may affect product quality, it has the potential to be applied for the controlled and immediate release of materials, particularly from double-emulsion droplets. The targeted release of microbials from double emulsions was discussed recently by Zhang et al. [19], who showed the promising application of this system whereby release can be triggered by various factors, which may help to enable applications in various food and drug environments. Previous studies also show an interesting application of emulsions for the controlled release of encapsulated materials with changes in temperature, which has good potential to be applied in industries such as food and pharmaceuticals [17,18,20,21]. However, it is crucial to understand the mechanism behind the release to widen the applications of this system for controlled release. This study focused on the application of emulsion droplets for bacterial encapsulation under cold-temperature storage. It aimed to investigate the encapsulation of bacteria within single W/O and double $W_1/O/W_2$ emulsion droplets, focusing on their stability and viability during cold storage. A flow-focusing microfluidic device was utilised for droplet formation, where the effects of temperature variations on droplet stability, bacterial viability, and the controlled release of bacteria were explored. The detrimental effects of cold temperature on bacterial viability and droplet destabilisation during storage remain a challenge. Therefore, this study is crucial and may provide valuable information on the suitability of emulsion droplets for bacterial encapsulation under cold-temperature storage. In addition, temperature-induced bacterial release from double water-in-oil-in-water emulsions was explored to further determine its potential in the controlled release of encapsulated materials.

2. Materials and Methods

2.1. Materials and Bacterial Cultures

Microfluidic device fabrication was performed using a Polydimethylsiloxane (PDMS) preparation set (Sylgard 184, Dow-corning, Midland, MI, USA), which included the curing agent and pre-polymer. The oil-soluble surfactant, polyglycerol polyricinoleate (PGPR), was obtained from Danisco (Copenhagen, Denmark). Soybean oil (Alfa Aesar, Lancashire, UK) was used as the oil phase for both single water-in-oil (W/O) and double water-in-oil-in-water ($W_1/O/W_2$) emulsion droplets. For bacterial culture preparation, the materials used were nutrient agar, Luria Bertani broth (LB broth), and phosphate-buffered saline (PBS), all from Oxoid Ltd. (Hampshire, UK). *Escherichia coli* strain SCC1 (MG1655-GFP mutation) expressing green fluorescent protein (*E. coli*-GFP) stock culture was obtained from the Biochemical Engineering Laboratory, University of Birmingham, United Kingdom.

2.2. Bacterial Cell Preparation

Bacterial cultures used for encapsulation in emulsion droplets were prepared by culturing *E. coli*-GFP on nutrient agar at 37 °C for 24 h. The cultured bacteria were kept at 4 °C prior to the experiment. The bacterial cells were then inoculated into 50 mL of Luria Bertani broth (LB Broth) in a shaking incubator at 37 °C and 150 rpm for 24 h, and then sub-cultured in fresh LB broth (1:50), followed by incubation for another 2 h. The bacterial culture was then centrifuged (10,000× g, 10 min) and washed two times with 50 mL of PBS. After centrifugation, the supernatant was discarded and replaced with 50 mL of fresh LB broth or DIW to re-suspend the bacterial cells for encapsulation. The bacterial cell concentration was prepared to 10^8 CFU/mL.

2.3. Microfluidic Device Fabrications

The microfluidic devices used for droplet generation were prepared using the standard soft lithography technique [22]. Device designs were based on specifications provided by Bauer et al. [23]. Patterned moulds were produced by printing the design onto high-resolution photomasks (Micro Lithography Services Limited, Essex, UK). Silicon wafers (Si-Mat, Kaufering, Germany) were spin-coated with SU-8 photoresist (SU-8, Microchem) and then exposed to UV light through the photomasks with a mask aligner (Canon PLA-501FA mask aligner, Canon, Tokyo, Japan). The PDMS mixture, consisting of PDMS and curing agent prepared at a recommended ratio of 1:10, was then poured onto the prepared mould, degassed, and cured in an oven at 70 °C for 1 h. The device was then cut out of the mould, and the inlet and outlet holes were punched, followed by corona discharge treatment (Relyon, PZ2) for approximately 30 s, which bonds the device onto a glass slide and seals the channels. The prepared device was then left on a hot plate for approximately 15 min at 100 °C. A new device was prepared for every experiment to minimise contamination.

As part of microfluidic device preparation, a partial hydrophilic surface treatment was performed on double-emulsion droplet devices to ease droplet formation [23]. Polyelectrolyte multilayers (PEM) consisting of alternating sequence of poly(allylamine hydrochloride) (PAH) and poly(sodium 4-styrenesulfonate) (PSS) solutions in 0.5 M of aqueous sodium chloride solution (0.1% w/v) was loaded into a Tygon tube (Cole-Parmer instrument Co. Ltd., Cambridge, UK) with 0.1 M of sodium chloride (NaCl) in deionised water as the washing solution. The PEM was then flushed through the lower part of the microfluidic device while the upper part was blocked with a stream of deionised water. At the end of the process, the lower part of the microfluidic channel was coated with PEM, rendering the channel walls hydrophilic while the upper part remained hydrophobic.

2.4. Microfluidic Encapsulation of E. coli-GFP in W/O and $W_1/O/W_2$ Droplets

The prepared culture of *E. coli*-GFP in deionised water (DIW) was then used as the aqueous phase of W/O and the inner aqueous phase of $W_1/O/W_2$ droplet. The oil phase for both types of emulsion consisted of soybean oil with 1.5% w/v PGPR surfactant, while for $W_1/O/W_2$, the outer aqueous phase consisted of DIW with 1% w/v Tween 80 surfactant. The bacterial encapsulation was conducted using a flow-focusing microfluidic device, whereby a single junction device was used for generating W/O droplets, while the encapsulation into $W_1/O/W_2$ was performed using a double junction device. The devices were connected to a pressure controller (OB1 MK3, Elveflow, Paris, France) to produce monodispersed droplets of approximately 50 µm in diameter for W/O. To generate a double emulsion, the W/O droplets were further emulsified with an outer aqueous phase, producing dispersed oil globules of approximately 100 µm in diameter. The produced droplets were collected in Eppendorf tubes for further analysis.

2.5. Storage of Samples at Different Temperatures

The prepared samples of emulsion droplets with or without *E. coli*-GFP were stored at different temperatures, 25 °C (control), 5 °C (refrigeration temperature), −20 °C (freezing

temperature), and −80 °C (freezing temperature), in laboratory-based refrigerators and freezers, with the temperature monitored throughout the storage period. Samples were stored for 24 h and thawed at 25 °C for 1 hour prior to further tests. Samples of *E. coli*-GFP suspended in sterilised deionised water (DIW) were also prepared and kept at the designated temperature as non-encapsulated controls.

2.6. Bacterial Viability Determination

The viability of *E. coli*-GFP was determined before and after the thawing process of samples stored in different temperatures. Encapsulated samples were centrifuged at 15,800× *g* for 1 min to break the emulsion and release the entrapped cells. Serial dilutions of the samples were performed using phosphate-buffered saline (PBS), and viable cells were counted immediately after sample preparation and after storage using the Miles and Misra method [24].

2.7. Microscopic Observation of Droplet Destabilisation

Droplet destabilisation was observed in relation to changes in temperature. The samples were prepared for microscopy by placing approximately one drop of sample onto the glass slide. The prepared glass slide was then placed on a Peltier temperature-controlled stage (Model PE-120, LINKAM scientific instruments, Surrey, UK), where the temperature of the stage was controlled using Link software (Linksys32, version 2.4.3). An Eheim circulation pump (ECP) was used for water circulation throughout the stage to maintain the desired temperature. The temperature-controlled stage was fitted on a Nikon Eclipse Ti microscope equipped with a Pco. Edge 5.5 sCMOS camera, where the samples were cooled and thawed on the microscope stage while photomicrographs of the samples were acquired. The sample was prepared at an initial temperature of 25 °C and was cooled down to −25 °C. The sample was then thawed to the initial temperature of 25 °C. For fluorescence microscopy, the encapsulated *E. coli*-GFP was observed at 509 nm emission.

2.8. Determination of Droplet Size and Phase Separation

The effect of different storage temperatures on droplet size was determined by measuring the diameter of the droplet immediately after sample preparation and after the thawing process at 25 °C. Single and double-emulsion samples without *E. coli*-GFP were prepared as controls. Photomicrographs of the droplet were taken before and after the storage period, and changes in the size of the dispersed aqueous phase for single-emulsion droplets and oil globule size for double-emulsion droplets were measured using MATLAB software (version 9.6, R2019a) and the circular Hough transform [25].

Droplet stability was also determined by measuring the amount of free water (for W/O emulsion) and free oil (for $W_1/O/W_2$ emulsion) with or without the presence of *E. coli*-GFP. Phase separation measurement was performed by collecting 1 mL of sample into graduated syringes immediately after droplet preparation. The samples were then stored at different temperatures in an upright position for 24 h. The volume of the free water and oil were measured from the graduated syringe immediately after the thawing process, and the percentage of free water and oil were determined as follows:

$$Percentage\ of\ separated\ water/oil\ (\%) = \frac{V_{water/oil}}{V_{emulsion}} \times 100$$

where $V_{water/oil}$ is the volume of separated water or oil measured from the graduated syringe, while $V_{emulsion}$ is the total volume of the emulsion sample.

2.9. Measuring the Release of Bacteria from $W_1/O/W_2$ Droplet

The release of bacteria was determined by measuring the number of cells in the outer aqueous phase immediately after sample preparation and after the thawing process of the double-emulsion samples ($W_1/O/W_2$). Samples stored in Eppendorf tubes were kept upright to allow the separation of the samples into a cream layer (oil globules) and serum

phase (W_2) due to the difference in density between the phases. The serum was then carefully withdrawn from the sample using a pipette and serially diluted in PBS. Plate counts were then performed according to the Miles and Misra [24] method, where the encapsulation efficiency was calculated following El Kadri et al. [26], and the percentage of released cells was quantified relative to the overall viable cells in the samples after storage as follows:

$$Encapsulation\ efficiency\ (\%) = \left(\frac{N_0 - N}{N_0}\right) \times 100$$

$$Bacterial\ release\ (\%) = \frac{Log_{10}N_1 - Log_{10}N_t}{Log_{10}N_1} \times 100$$

where N is the number of viable cells counted in the serum phase immediately after emulsion preparation and N_0 is the overall viable cell count prior to encapsulation in $W_1/O/W_2$ droplets. N_1 is the overall viable cells after storage, and N_t is the viable cell count in the serum phase after storage at temperature t.

2.10. Differential Scanning Calorimetry

Differential scanning calorimetry (DSC) was performed to determine the thermal properties of emulsions samples and bulk aqueous solutions. The crystallisation and melting behaviours were characterised using a differential scanning calorimeter (Mettler Toledo, model 822e, Mettler Scientific Instruments, Giessen, Germany) with liquid nitrogen as the cooling substance. Approximately 5 mg of sample was weighed and hermetically sealed in aluminum pans together with an empty pan as reference. Samples were then cooled from 25 °C to −70 °C and held at −70 °C for 5 min before being heated back to 25 °C at a rate of 1 °C/min. The cooling and heating curves were obtained using STARe software version 9.0 (Mettler Toledo, Mettler Scientific Instruments, Germany), whereby positive curves resulted from an exothermic reaction, while an endothermic reaction created negative curves. The crystallisation and melting points of the tested samples were determined from the peak onset temperatures of the curves using the same software.

2.11. Statistical Analysis

All experiments were conducted with three replicates (n = 3). The data obtained were analysed with Excel (Microsoft corp., Washington, DC, USA) to determine the mean, standard deviation (SD), and standard error of means (SEM). A one-way ANOVA with Tukey HSD was conducted to compare several means, while a Student's t-test was conducted to compare two means using IBM SPSS Statistical software, version 23. Differences between means were considered significant at $p < 0.05$.

3. Results and Discussion

3.1. The Effect of Storage on Droplet Size Change

Monodisperse droplets for both single- and double-emulsion droplets were observed for all samples, with or without *E. coli*-GFP, with a CV value of approximately 9% for single-emulsion droplets and 7% for double-emulsion droplets prior to the storage test, as observed in Figure 1A,C,E,G and Table 1. The results indicate the ability of the flow-focusing microfluidic devices to produce highly monodisperse droplets, and the presence of *E. coli*-GFP did not affect droplet formation. For samples of single-emulsion droplets, no significant change ($p > 0.05$) in droplet size was observed after storage at 25 °C and 5 °C (Table 1) for both samples with and without bacteria. The droplets remained monodisperse, with only a 0.1–0.2% change in the value of the coefficient of variation (CV). However, a significant change ($p < 0.05$) in droplet size and distribution was observed after 24 h of storage for samples stored at freezing temperatures of −20 °C and −80 °C for both samples with and without bacteria. The greatest change was observed for samples stored at −80 °C, where the CV value increased from 9.6% to 28.3% for samples without *E. coli*-GFP, indicating a polydisperse distribution of droplets (CV values greater than 25% are regarded as polydisperse). Comparing samples with or without *E. coli*-GFP, the change in

droplet stability was minimised in the presence of *E. coli*-GFP, whereby a smaller change in average droplet size and CV was observed with samples containing *E. coli*-GFP compared to samples without *E. coli*-GFP.

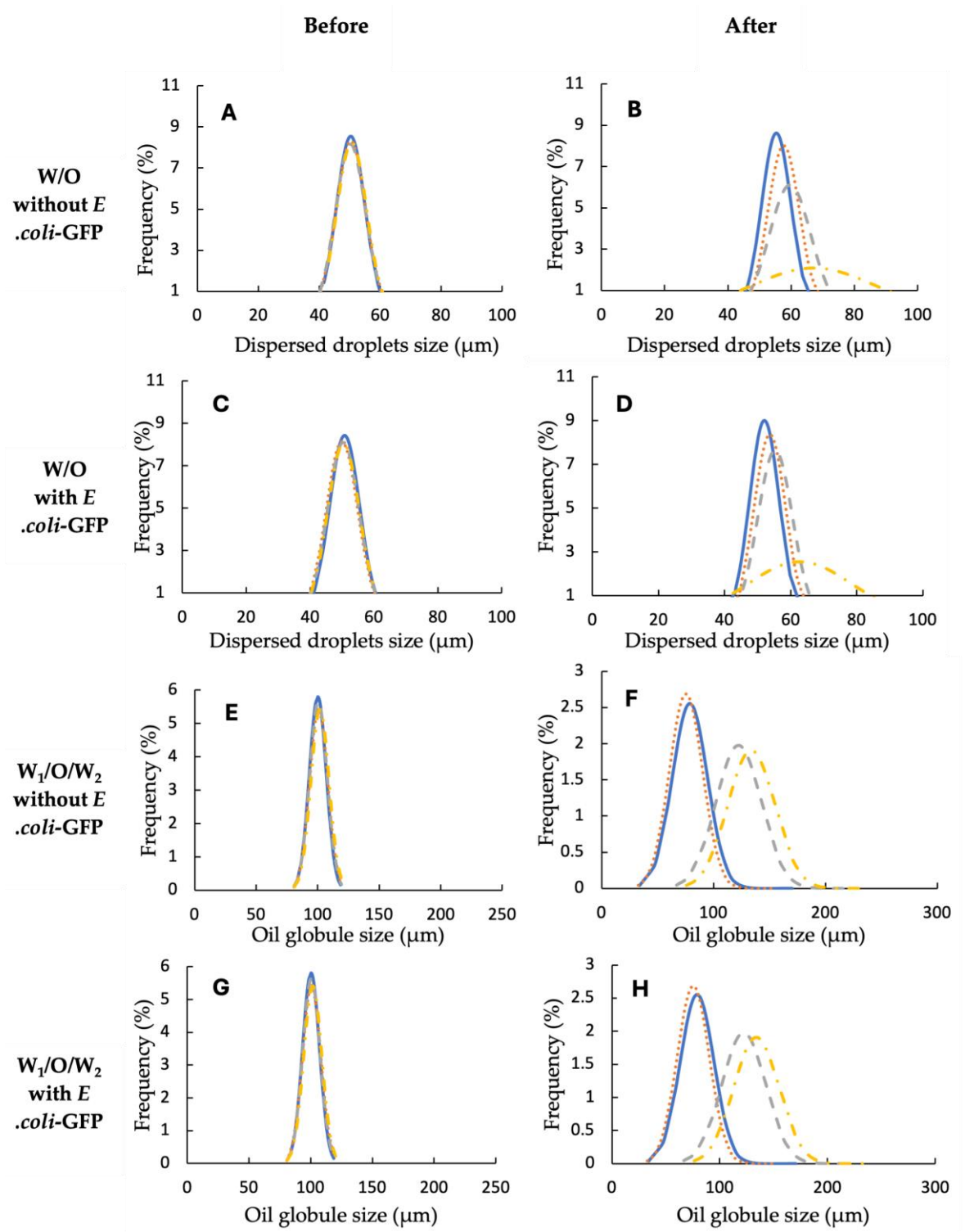

Figure 1. Droplet size distribution for single W/O (**A**–**D**) and double $W_1/O/W_2$ (**E**–**H**) emulsions at 25°C (—), 5°C (⋯), −20°C (----), and −80°C (- · -) before and after 24 h of storage. Droplet size measurements were taken after the samples were allowed to reach 25 °C following storage at cold temperatures.

Table 1. Summary of droplet size and distribution measured before and after 24 h of storage. Samples were prepared with or without *E.coli*-GFP for W/O and W1/O/W2 droplets. Data represent the mean ± standard deviation taken from three independent experiments with N = 900 droplets. The coefficient of variation (%) was measured by dividing the standard deviation by the mean droplet diameter. Mean comparisons indicated by small letters and capital letters represent significant differences ($p < 0.05$) within each sample across temperatures and before and after storage at each temperature, respectively. Data were analysed using one-way ANOVA and Student's *t*-test.

Samples	Temperature (°C)	Average Droplet Diameter (μm)		Coefficient of Variation (%)	
		Before	After	Before	After
W/O without *E. coli*-GFP	25	50.4 ^{aA} ± 4.7	55.3 ^{aA} ± 5.2	9.3	9.4
	5	50.4 ^{aA} + ± 4.8	57.7 ^{aA} ± 5.6	9.5	9.7
	−20	50.3 ^{aA} ± 4.9	59.6 ^{cB} ± 6.6	9.7	11.1
	−80	50.7 ^{aA} ± 4.8	67.2 ^{dB} ± 19.0	9.6	28.3
W/O with *E. coli*-GFP	25	50.8 ^{aA} ± 4.7	52.1 ^{aA} ± 4.9	9.3	9.4
	5	50.0 ^{aA} ± 4.9	53.7 ^{aA} ± 5.3	9.8	9.9
	−20	50.4 ^{aA} ± 4.9	55.3 ^{bB} ± 5.4	9.7	9.8
	−80	50.5 ^{aA} ± 5.0	62.8 ^{cB} ± 15.6	9.9	24.8
$W_1/O/W_2$ without *E. coli*-GFP	25	100.3 ^{aA} ± 6.9	79.0 ^{aB} ± 15.6	6.9	19.7
	5	100.7 ^{aA} ± 7.3	75.4 ^{bB} ± 14.9	7.2	19.8
	−20	100.6 ^{aA} ± 7.1	122.3 ^{cB} ± 20.2	7.1	16.5
	−80	101.8 ^{aA} ± 7.4	133.8 ^{dB} ± 20.9	7.3	15.6
$W_1/O/W_2$ with *E. coli*-GFP	25	100.9 ^{aA} ± 7.1	79.4 ^{aB} ± 15.6	7.0	19.6
	5	100.3 ^{aA} ± 7.7	76.3 ^{bB} ± 14.7	7.7	19.3
	−20	100.4 ^{aA} ± 7.1	116.7 ^{cB} ± 18.5	7.1	15.9
	−80	100.4 ^{aA} ± 7.4	126.3 ^{dB} ± 18.9	7.4	14.9

A significant change ($p < 0.05$) in the size of oil globules after 24 h of storage was observed for all double $W_1/O/W_2$ emulsion samples, with a decrease in average oil globule size observed for samples stored at 25 °C and 5 °C. However, the presence of large droplets up to 170 μm in size was also observed (Figure 1F,H). For samples stored at freezing temperatures of −20 °C and −80 °C, an increase ($p < 0.05$) in droplet size after storage was noted (Table 1). Samples containing *E. coli*-GFP demonstrated better droplet stability compared to those without, indicating the ability of bacterial cells to maintain droplet stability during cold-temperature storage. Complete external coalescence occurred between the inner W_1 droplet and the outer W_2 phase after 24 h of storage, forming a single oil-in-water (O/W) emulsion.

The storage of single W/O samples at −20 °C resulted in the solidification of the aqueous phase and partial crystallisation of the oil phase, whereas storage at −80 °C completely solidified the emulsions. With a broad crystallisation temperature, as opposed to pure water, which exhibits a sharp crystallisation curve, it is quite difficult to determine the exact crystallisation temperature of soybean oil due to the presence of lipids and a mixture of molecules. It has been reported previously that soybean oil is partially crystallised at a temperature between −10 °C and approximately −20 °C, whereby below this temperature, soybean oil is most likely to become solid [27–30].

Several destabilisation mechanisms of single W/O emulsions during the freeze–thaw process have been proposed, depending on droplet arrangements in the emulsion [16,31–34]. The destabilisation of loosely packed W/O emulsion droplets is due to collision-mediated coalescence [16]. This process is triggered by the uneven crystallisation of polydisperse

water droplets in the emulsion, whereby the collision between the smaller, still-liquid water droplet and protruding ice crystals of the larger frozen droplet punctures the membrane surrounding the smaller, still-liquid water droplet. This leads to heterogeneous nucleation, with smaller droplets coalescing to form larger droplets upon thawing [16,35]. However, this may not be the case for a single W/O droplet generated using the microfluidic device, as it is highly monodispersed and therefore minimises the heterogeneous crystallisation of the water droplet and the effect of collision-mediated coalescence. Although the effect of collision-mediated coalescence was minimised, the destabilisation of W/O droplets was still observed, which is mainly attributed to the static and upright storage of the samples during freezing that caused the inevitable sedimentation of the water droplets, making them closely packed. For densely packed emulsions, the destabilisation mechanism is induced by the direct breakage of interfacial films and emulsion inversion [31,32]. The direct breakage of the droplet interfacial film occurred as neighbouring droplets crystallised and expanded, causing destabilisation. Droplet expansion pressed the droplets closely together, while crystallised droplets punctured the interfacial film of neighbouring still-liquid droplets, leading to droplet rupture [14]. This caused the content of the ruptured droplet to flow out and form a link between the two frozen droplets, resulting in flocculation, as observed in this study in Figure 2b [36]. During the thawing process, the crystal network collapsed, and the two partially coalesced droplets merged together, forming a larger droplet (complete coalescence), as observed in Figure 2d [12]. Droplet crystallisation and expansion also resulted in the thinning of the oil and surfactant layer around the aqueous phase, which accelerates droplet coalescence during the melting process [35]. Emulsion inversion, as reported by Aronson and Petko [31], involves the rearrangement of ice crystals and the still-liquid oil, which leads to the presence of distinct oil droplets within the ice structure. However, this may not be the case for samples tested in this study, as it occurs mainly in densely packed emulsions containing distinctively high-volume fractions of the dispersed phase [12].

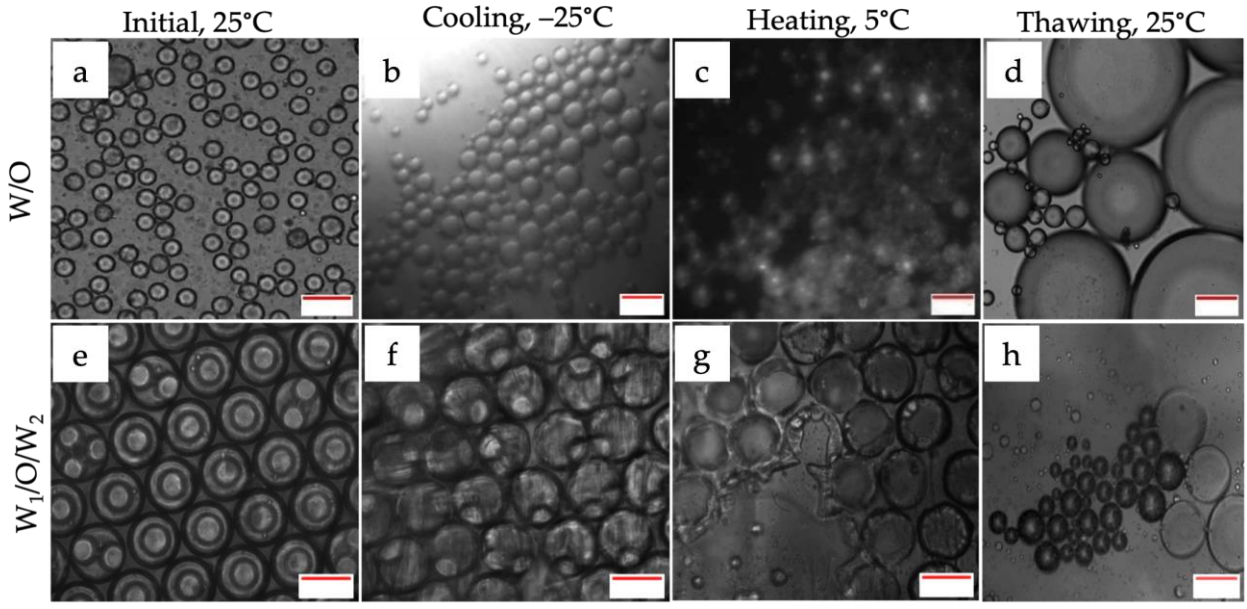

Figure 2. Photomicrographs of W/O (**a**–**d**) and $W_1/O/W_2$ (**e**–**h**) emulsion droplets with change in temperature. The cooling and thawing processes were conducted on the temperature-controlled microscope stage. Scale bar represents 100 µm.

It has been reported previously that the stability of water-in-oil droplets during the freeze–thaw process depends on the freezing sequence of the oil and aqueous phases and also the type of surfactants used [35]. The freezing sequence between the oil and aqueous phase may depend on the type of oil used, as some oils may have a lower or higher freezing

point than the aqueous phase. Ghosh and Coupland [14] reported that for single water-in-oil emulsions, instability is mostly evident in samples where the oil phase crystallises first prior to the aqueous phase and when the emulsifier is in a liquid state during the freezing process. For emulsions containing soybean oil, the oil phase crystallises at a much lower temperature than the aqueous phase, minimising droplet destabilisation. However, significant changes ($p < 0.05$) in droplet size distribution were observed for samples stored at −80 °C. At −80 °C, the gradual crystallisation of the oil phase occurs due to differences in the melting fraction of fats in soybean oil, as the high-melting fraction crystallises first, followed by the low-melting fraction [30], resulting in ice crystals being forced into the still-liquid oil phase forming a region with highly concentrated ice crystals [14,37]. During thawing, as the oil melts, the ice crystals coalesce immediately, as a further increase in temperature causes the aqueous droplets to melt and fuse together [38]. A previous study reported the separation of the W_1 phase from double-emulsion droplets, where the separated W_1 phase was retained in the W_2 phase supported by a very thin and complex layer of oil and surfactants [39]. This also caused the reduction in oil globule size as the W_1 phase escaped into the W_2 phase. Similar behaviour was also seen for samples with double emulsions kept at a lower temperature of 5 °C. However, for double-emulsion samples kept at a much lower temperature of −20 °C and −80 °C, a significant ($p < 0.05$) increase in the average oil globule size and change in the droplet size distribution was observed. Interestingly, the inner W_1 phase remained intact in the $W_1/O/W_2$ during the freezing process, as shown in Figure 2f, and the droplet separation process was not observed.

The destabilisation mechanism of the double-emulsion droplets was primarily attributed to external coalescence between the W_1 and W_2 phases, a process distinct from the freeze–thaw destabilisation of single emulsions [17,40]. In contrast to single-emulsion droplets, whereby the droplet destabilisation process occurs throughout the freeze and thawing processes, the external coalescence of double emulsions occurred during the thawing process of the emulsions, while the inner W_1 phase remained intact during the freezing process [17]. The thawing process caused deformation of the inner W_1 phase followed by the complete burst of the droplet due to the external coalescence, and this process is mainly affected by the size of the inner W_1 phase and surfactant concentration. According to Rojas and Papadopoulos [17], the determined threshold of the W_1 inner aqueous phase size to the oil globule size ratio is 0.3, above which coalescence occurs upon thawing. In addition, an emulsion droplet with a thick surfactant layer creates a repulsive force between the W_1 inner phase and the O/W_2 interface that improves droplet stability against external coalescence [41]. A similar mechanism was observed in this study, whereby the inner W_1 droplet remained intact during the freezing process and rapid freezing prevented the droplet from splitting (Figure 2e–f). Emulsion destabilisation only occurred during the thawing process for both samples kept at −20 °C and −80 °C. As the frozen oil melts at a lower temperature during the thawing process of samples kept at freezing temperatures, the liquid oil flows through the cracks and gaps created by the gradual thawing of the aqueous phase (Figure 2g), leading to the absence of the oil layer that separates the inner W_1 phase from the outer W_2 phase. This accelerates the external coalescence of the aqueous phase, as it melts completely with an increase in temperature, forming a single oil-in-water (O/W) emulsion. Moreover, the droplet distribution graph that tails towards the larger droplet size with sharp distribution in the smaller droplet size region shows evidence of oil globule coalescence after the thawing process, which contrasts with droplet instability that was induced by Ostwald ripening, whereby it tends to form a sharp droplet distribution in the larger region with tailing in the smaller droplet size region [31].

The presence of bacteria also affected droplet stability, especially for single-emulsion droplets. As the PGPR surfactant remained liquid during the freezing process [35], it is most likely retained in the oil phase and withdrawn from the ice crystals as the aqueous phase freezes. This accelerates the coalescence process of the aqueous phase as the emulsions warm up. However, the presence of *E. coli*-GFP on the interface minimises droplet coalescence during the thawing process as it is most likely crystallised on the interface. *E.*

coli-GFP was observed to have a high affinity towards the soybean oil, as determined by the BATH assay (Figure S2). Changes in bacterial characteristics due to storage in freezing temperatures ease the attachment of the bacteria onto the interface, making the droplet less susceptible to rupture. The stabilisation effect of bacteria may be similar to emulsion stabilisation due to surfactant crystallisation and the presence of particles on the droplet interface forming Pickering emulsions, as reported previously [34,41]. It has been reported previously that the crystallisation of glycerol monostearate (GMS) at 25 °C creates a crystalline shell around the water droplet that helps prevent crystallisation damage between the adjacent water droplets and reduces coalescence during the thawing process, which is in contrast to emulsions containing molten PGPR [35]. According to Zhu et al. [42], the addition of heated soy and whey protein in emulsions improves droplet stability against freeze/thaw cycling due to Pickering stearic stabilisation. However, further studies are still required to confirm the effect of bacteria on droplet stability in freezing conditions.

Recent studies applied numerical and computational models to understand the formation and stability of emulsion droplets in micro-fluidic channels without bacteria [43,44]. Furthermore, since bacteria have an impact on emulsion formation and stability, in future, numerical and computational studies can simulate this complex interaction to optimise the formation of emulsions encapsulating bacteria by predicting conditions that lead to the desired size and stability and to develop an efficient and scalable system for various applications.

3.2. The Effect of Storage on Phase Separation of Emulsions

Droplet destabilisation of W/O droplets resulted in the presence of a free water layer due to droplet coalescence, while the destabilisation of $W_1/O/W_2$ droplets led to the presence of a free oil layer due to the external coalescence between the inner and outer aqueous phases (forming an O/W emulsion) and coalescence between large oil droplets that resulted in the presence of an oil layer on top of the sample. Figure 3 shows the percentage ratio of free water and oil measured after 24 h of storage with respect to the total emulsion. Given the results obtained, it was determined that phase separation occurred for samples of both single and double emulsions kept at −20 °C and −80 °C, with the highest amount of free water and free oil observed for samples kept at −80 °C. Emulsion stability for samples stored at 25 °C was maintained during the storage period, as there was no observable free water or oil. However, a small percentage of free water and oil (approximately 2%) was observed for samples without *E. coli*-GFP at 5 °C, and this is mainly attributed to the closely packed water droplets during storage and the absence of *E. coli*-GFP that helped in improving droplet stability. An overall comparison between samples with or without the presence of *E. coli*-GFP shows that phase separation was minimised with the presence of *E. coli*-GFP.

Droplet destabilisation occurred for W/O emulsions kept at −20 °C and −80 °C due to partial coalescence of the droplets, as the crystallisation of the dispersed phase resulted in film rupture that connected neighbouring droplets, leading to complete coalescence upon thawing [12,45]. This eventually led to bulk water separation that was minimised with the presence of *E. coli*-GFP in the inner W_1 phase. During the consecutive crystallisation of the oil phase, the dispersed ice crystals were forced into the still-liquid region of the oil phase, and a further reduction in temperature led to the withdrawal of crystallised oil from this region. A combination of these processes led to complete droplet coalescence and extensive aqueous phase separation from the emulsion during the thawing process [37,38]. The partially crystallised oil phase of samples stored at −20 °C prevented the complete withdrawal of the oil phase, as some regions within the emulsion contained liquid oil, thus minimising extensive droplet coalescence.

The direct destabilisation process of the double-emulsion droplet that occurs immediately after the thawing process leads to oil phase separation and the external coalescence of W_1 and W_2 phases. As shown in Figure 2g, the movement of liquid oil through the cracks of the outer aqueous phase during the thawing process immediately separates the oil and aqueous phases, forming a bulk oil layer due to the coalescence of bigger oil droplets, while

some oil droplets remain in a layer of O/W emulsion. The unfrozen W_1 phase will remain in the W_2 phase and eventually fuses with the W_2 phase as it melts (Figure 2h). This process leads to the complete release of the W_1 phase into the W_2 phase and extensive separation of the oil phase from the emulsion. Complete $W_1/O/W_2$ emulsion destabilisation due to external coalescence during the thawing phase of the oil layer was also reported previously by Rojas and Papadopoulos [17], whereby it led to the complete release of the W_1 phase into the W_2 phase, forming O/W emulsions.

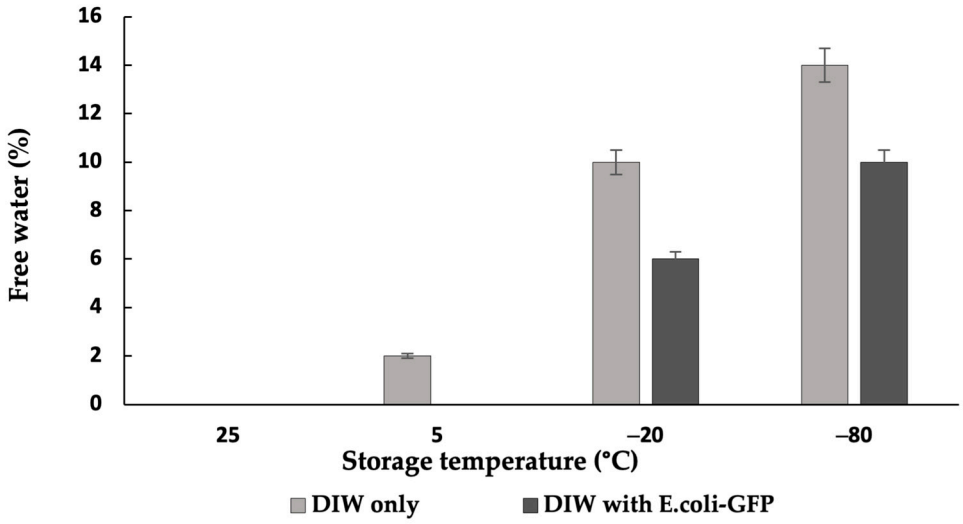

(**a**)

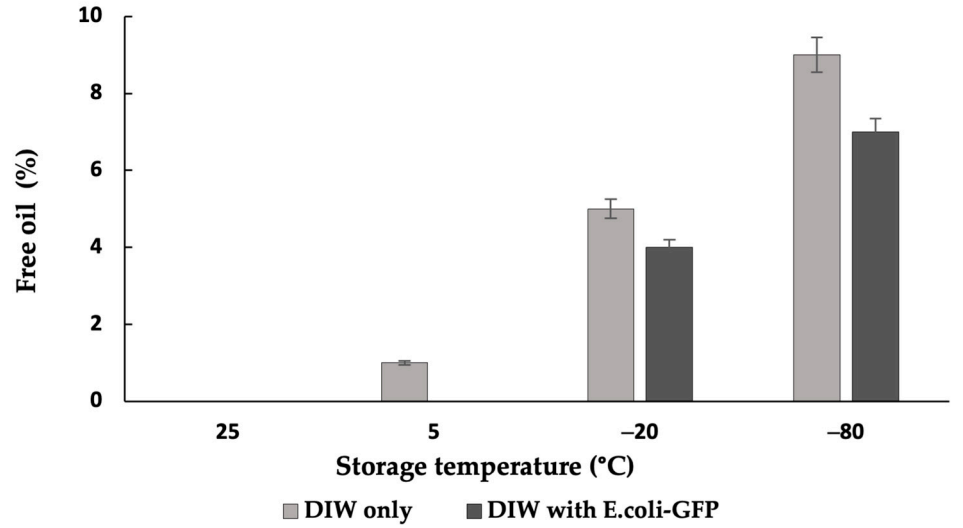

(**b**)

Figure 3. The percentage of (**a**) free water measured for single-emulsion samples and (**b**) free oil for double-emulsion samples. The volume of free water and free oil was measured with respect to the total volume of emulsions after 24 h of storage at different temperatures. Bars represent the mean ± SEM obtained from 3 independent experiments.

The presence of crystallised surfactants and Pickering particles has been reported to improve droplet stability, as it minimises droplet coalescence during the thawing process by creating a protective layer that prevents droplet fusion [14,42,46]. A similar stabilisation effect may occur with the presence of *E. coli*-GFP on the interfacial layer. Under freezing conditions, *E. coli*-GFP undergoes changes in membrane conformation and cell shrinkage [47], making it easily embedded in the interfacial layer. A previous study reported

that the presence of *E. coli*-GFP in single W/O emulsion droplets helps in maintaining the stability of the droplet during five days of storage at 25 °C, whereby the presence of *E. coli*-GFP, particularly dead cells, helps in reducing interfacial tension due to its attachment on the interfacial layer [48]. The bacterial affinity for the interface is due to its hydrophobic nature, as the dead *E. coli*-GFP cells exhibit a higher affinity for the oil phase compared to live cells. The BATH assay of *E. coli*-GFP with soybean oil reveals its affinity for the oil phase (Figure S2); thus, this may help to reduce the interfacial tension and create a protective barrier that prevents extensive droplet coalescence during the thawing process. Moreover, the presence of bacteria in the W_2 phase due to its release as the $W_1/O/W_2$ emulsion destabilises may help prevent coalescence between the oil droplets, as reported previously by Firoozmand and Rousseau [49], whereby the presence of bacterial cells in the aqueous phase of the O/W emulsions improves droplet stability due to the attachment of bacterial cells onto the oil droplets, creating a boundary layer that protects the droplet against coalescence and phase separation.

3.3. Thermal Properties of Emulsions Determined Using Differential Scanning Calorimetry (DSC)

The thermal properties of the bulk aqueous solution (Figure 4) were characterised as opposed to emulsified samples of single and double emulsions in soybean oil (Figure 5). The crystallisation temperature of the samples was determined from the onset temperatures of the crystallisation peaks in which the temperature was recorded at the beginning of the crystallite formation. The onset temperature was determined by using Star e software version 9.0 (Mettler Toledo, Mettler Scientific Instruments, Giessen, Germany). Referring to the crystallisation peaks in Figure 4a, it was determined that the crystallisation of *E. coli*-GFP suspension in DIW occurred at a lower temperature compared to pure DIW. Pure DIW crystallises at −12 °C and melts at 0 °C, which is around the same temperatures as reported previously in several studies [13,35,50]. For the *E. coli*-GFP suspension, the crystallisation temperature was recorded at −17 °C, while the melting of the *E. coli*-GFP suspension occurred around the same temperature as the pure DIW. The reduction in the crystallisation temperature with the presence of *E. coli*-GFP is due to the freezing point depression, where the presence of *E. coli*-GFP as a solute tends to lower the freezing point.

Figure 5 shows that the emulsified samples freeze at a much lower temperature compared to bulk solutions. A broader crystallisation curve was observed for samples of W/O emulsions as compared to $W_1/O/W_2$ emulsions. This is mostly attributed to the presence of a large percentage of oil in the continuous phase as compared to the aqueous phase for W/O emulsions. The presence of long chains of lipids together with a mixture of other molecules in soybean oil results in a broader crystallisation temperature as opposed to pure water, making it difficult to determine the exact freezing point of the soybean oil. It has been reported that pure soybean oil crystallises at approximately −10 °C to −20 °C, where it is most likely to solidify below these temperatures, while soybean oil emulsions solidify at a much lower temperature than pure oil [28,30]. In this study, the single W/O emulsion crystallised at −20 °C for samples without *E. coli*-GFP, while samples with *E. coli*-GFP crystallised at −28 °C. The melting point of both emulsions was around 0 °C. The difference in crystallisation temperature is mainly attributed to the destabilisation of emulsions without *E. coli*-GFP, where the presence of free water due to phase separation increases the crystallisation temperature of the samples. In addition, the similar melting point of the emulsions as that of bulk solutions also indicates the loss of emulsion stability due to an increase in the percentage of free water during the thawing process [34,50]. It has been reported previously that the W/O emulsions solidify at a lower temperature than that of bulk water as they overcome the free energy barrier due to homogeneous nucleation [12]. Water droplets in emulsions solidify at a lower temperature than the temperature required to solidify bulk water (−20 °C) and are much lower than the equilibrium melting point of water of 0 °C [16].

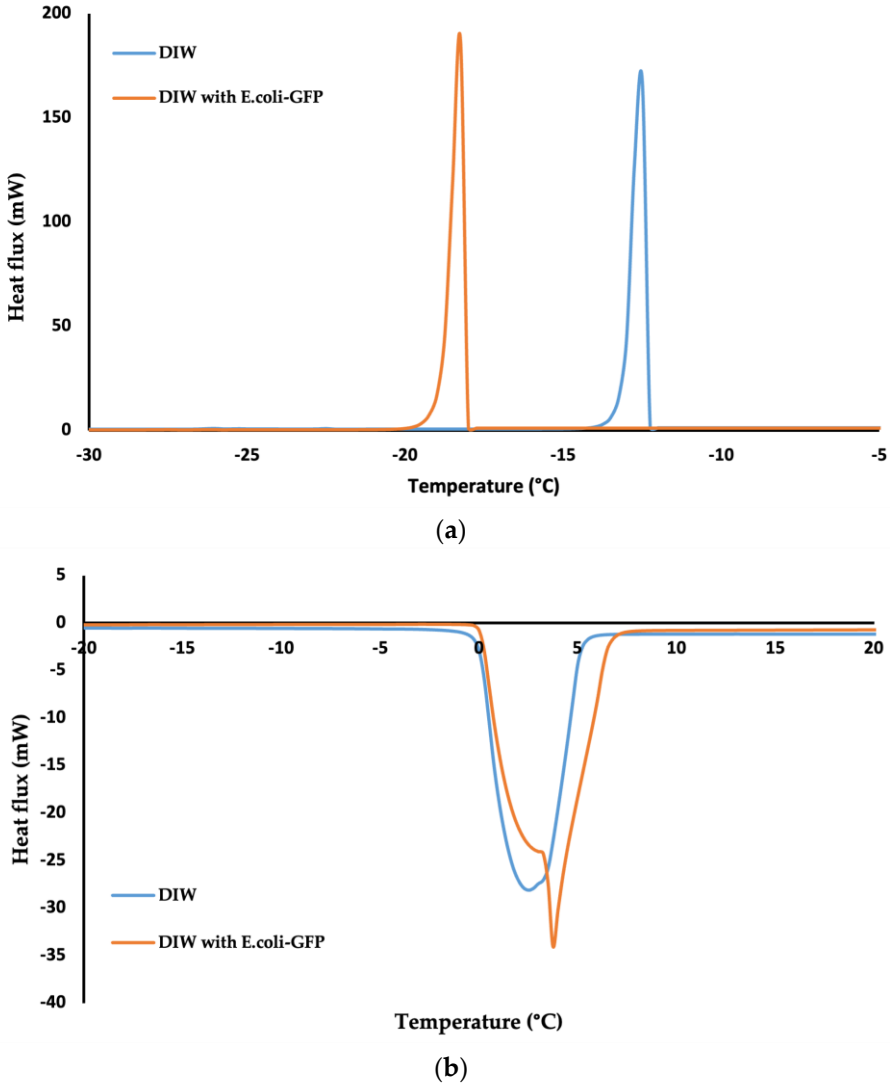

Figure 4. DSC thermograms showing the cooling curves (**a**) and heating curves (**b**) of bulk aqueous samples with or without *E. coli*-GFP.

For double $W_1/O/W_2$ emulsions, a small difference in crystallisation temperature was observed between samples with or without *E. coli*-GFP, as samples containing *E. coli*-GFP crystallised at −21 °C while samples without *E. coli*-GFP crystallised at −23 °C. Only one peak was observed, which represents the crystallisation peak of the W_2 phase as opposed to the two peaks reported by Kovács et al. [51]. The absence of the second peak indicates the loss of the inner W_1 phase due to emulsion breakdown [51,52]. However, this may not be the case in this study, as the inner W_1 droplets were intact during the freezing process, as observed in Figure 2f, and the loss of the inner W_1 phase occurred during the thawing/melting process, which explains the presence of only one peak for the melting curve with a melting temperature of approximately 0 °C for all samples. Schuch, Köhler and Schuchmann [52] also described that it is possible to distinguish between the inner W_1 phase and the outer W_2 phase from the cooling curves due to the presence of two peaks that result from the difference in crystallisation temperatures, but it is impossible to distinguish between these two phases from the melting curves of the $W_1/O/W_2$. Another possible explanation for the presence of only one cooling curve is due to the highly monodispersed distribution of the droplets that were prepared by using the microfluidic method with a single and large size W_1 core and a thin oil layer separating the W_1 phase from the W_2 phase. A combination of these factors may have caused the outer W_2 phase and the inner W_1 phase to crystallise simultaneously within the same temperature range. It has been

reported previously that the crystallisation of emulsion droplets may depend on the size of the droplet [52]. However, further studies are still required to understand the effect of the droplet size distribution on the crystallisation temperature of multiple emulsions.

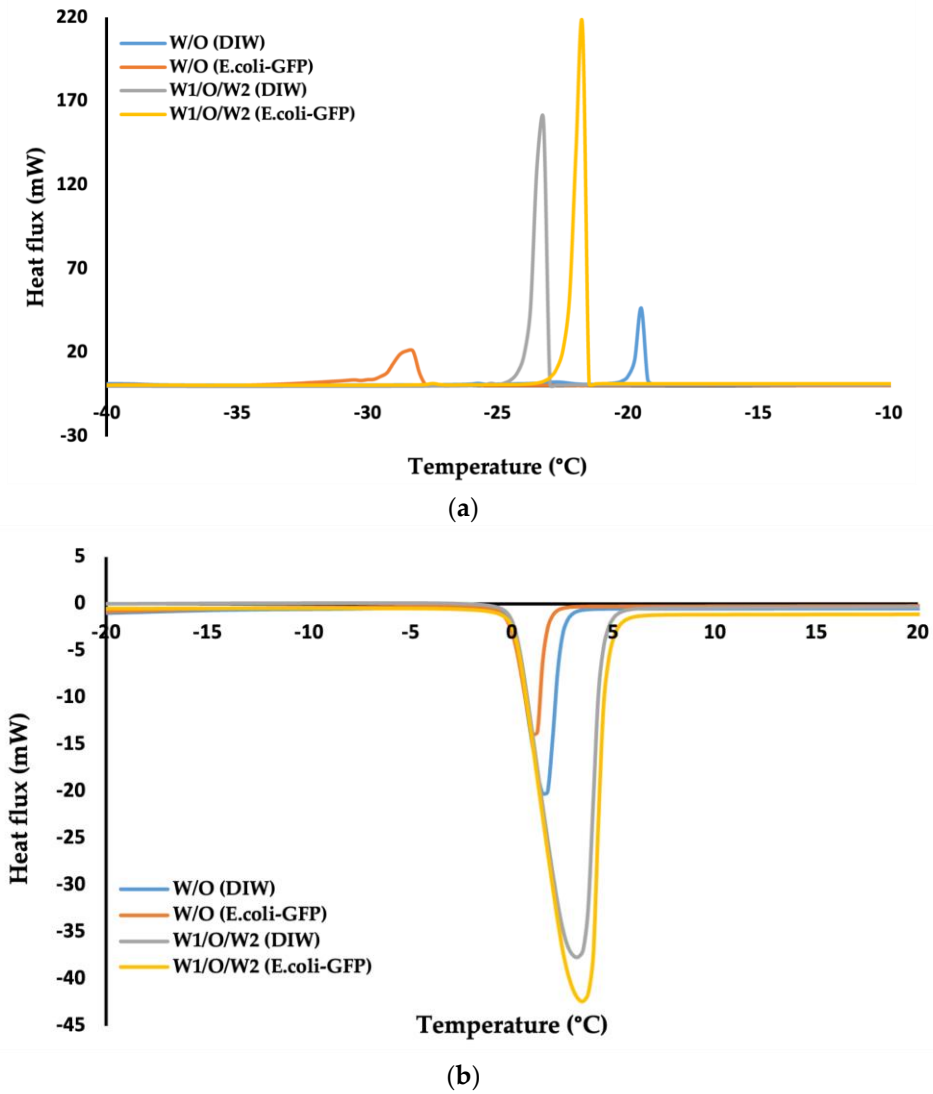

Figure 5. DSC thermograms of (**a**) cooling curves and (**b**) heating curves of emulsified samples with or without *E. coli*-GFP.

3.4. Bacterial Viability During Storage

Referring to Figure 6, a large reduction in the *E. coli*-GFP cell count was observed for samples kept at −20 °C and −80 °C compared to samples kept at 25 °C and 5 °C, whereby, comparing the non-encapsulated samples, a 1.2 log CFU/mL and 1.3 log CFU/mL reduction in viable cell count was observed for samples kept at 25 °C and 5 °C, respectively, while reductions of 2.3 log CFU/mL and 2.7 log CFU/mL were observed for samples kept at −20 °C and −80 °C, respectively. *E. coli*-GFP encapsulated in W/O droplets showed a smaller percentage of bacterial reduction compared to samples encapsulated in $W_1/O/W_2$ droplets and control samples of free *E. coli*-GFP cells in sterilised DIW.

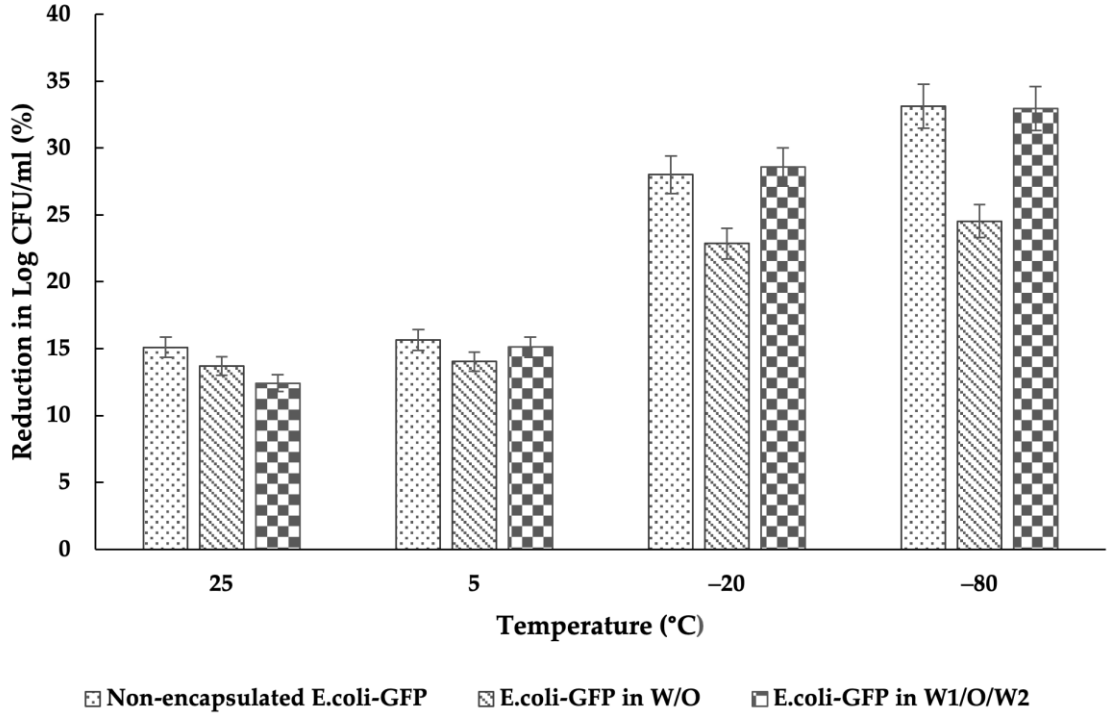

Figure 6. Reduction in Log CFU/mL of free *E. coli*-GFP in sterilised DIW and encapsulated in W/O or $W_1/O/W_2$ emulsion droplets. Bars represent mean SEM taken from 3 independent experiments.

It has been reported previously that freeze–thawing may cause detrimental effects on bacterial cells that lead to a reduction in bacterial viability [47,53–55]. Cell damage during the freeze–thaw process occurs due to various physico-chemical reactions [7,56]. One of the factors responsible for cell damage during storage at low temperatures is the nature of the cells [7,57], whereby different bacterial species exhibit different resistance to cell damage depending on the cell structure. Furthermore, the use of cryoprotectants with various formulations [7] and the freeze–thawing conditions [6,58] of the samples may also affect the degree of cell damage during storage.

The effect of water crystallisation is one of the most common factors responsible for cell damage [47,58,59]. The detrimental effect of water crystallisation on bacterial viability depends on the freezing rate, whereby the decrease in bacterial viability is minimised at a low freezing rate compared to a high freezing rate. This is due to the cryoconcentration effect, as the crystallisation of the external medium resulted in cell dehydration, thus preventing lethal intracellular crystallisation. Crystallisation of the extracellular medium forces the cells to be concentrated in the unfrozen region of the medium, whereby a continuous decrease in temperature causes the region to be increasingly concentrated. This leads to cell dehydration as the cells are exposed to a highly concentrated solution during the freezing process. Meanwhile, the rapid freezing of bacterial suspension resulted in extensive supercooling that crystallised intracellular water, as it was not able to flow out of the cells fast enough, causing extensive cell damage [56]. These findings indicate that the degree of cell damage during the freezing process depends on the availability of intra- and extracellular water. Referring to the DSC thermograms (Figure 5), the broader crystallisation temperature of the emulsion compared to the bulk bacterial solution (Figure 4) indicates that the encapsulation of bacteria in emulsion droplets promotes slow freezing and thus minimises cell damage during the freezing process. Encapsulation in W/O emulsion droplets shows a smaller reduction in cell count compared to samples encapsulated in $W_1/O/W_2$ emulsion droplets and free cells in DIW due to the thick oil layer and the low water ratio that minimises cell damage due to water crystallisation.

The effect of encapsulation in improving bacterial viability during the freeze–thaw process has also been reported previously [8,9,60]. The microencapsulation of *Lactobacillus*

acidophilus in the self-assembled polyelectrolyte layers of chitosan and carboxymethyl cellulose has been reported to protect bacteria not only from the adverse effects of the simulated GI tract but also during the freezing and freeze-drying processes [60]. Furthermore, the microencapsulation of *Bifidobacterium longum* in milk proteins and sugar alcohols aids in improving the protection effect of cryoprotectants such as glycerol, resulting in better bacterial viability and function after freezing and freeze-drying processes [9].

Moreover, the freezing of emulsion-based products such as milk has also been reported to cause small changes in the viability of bacteria, indicating the ability of the emulsion structure to protect bacteria against extensive cell damage. A study conducted by Sánchez et al. [61] shows that the freezing of goat milk at −20 °C or even after extended storage at −80 °C does not significantly affect the viability of *E. coli* as opposed to cow milk due to differences in milk composition. A similar result was also reported by Nurliyani, Suranindyah, and Pretiwi [10], whereby the frozen storage of Ettawah Cross-bred goat milk samples for 60 days did not cause significant changes in the total bacteria, while changes in emulsion stability were observed after 30 days of storage.

Therefore, the encapsulation of bacteria in emulsion droplets, especially W/O, may help in improving bacterial viability during the freezing process due to the protective effect of the emulsion structure, as it reduces the available water ratio and prevents the lethal crystallisation effect of the water phase.

3.5. The Release of Bacteria from Double Emulsions

Although the storage of samples at freezing temperatures leads to unfavourable phase separation, the immediate destabilisation of the $W_1/O/W_2$ emulsion triggered by the thawing process may be beneficial for the controlled release of bacteria for various applications. A high encapsulation efficiency of approximately 99% was achieved by using microfluidics for bacteria encapsulation in $W_1/O/W_2$, indicating the successful encapsulation of bacteria prior to cold storage. The increase in cell counts in the W_2 phase, therefore, resulted from the release of bacteria from the W_1 phase due to the emulsion destabilisation process during storage, as presented in Table 2.

Table 2. The effect of storage temperature on the release of bacteria from $W_1/O/W_2$ droplets. Samples were prepared with 99.9% encapsulation efficiency, and the release of bacteria into the W_2 phase was determined after 24 h of storage. Data represent mean ± standard deviation taken from 3 independent experiments.

Temperature (°C)	Overall Viability (log CFU/mL)	Released (log CFU/mL)	Released (%)
25	6.42 ± 0.03	2.75 ± 0.02	42.80 ± 0.51
5	6.18 ± 0.01	2.77 ± 0.01	44.89 ± 0.23
−20	5.19 ± 0.02	5.10 ± 0.01	98.36 ± 0.18
−80	4.93 ± 0.03	4.90 ± 0.01	99.35 ± 0.40

Complete bacterial release into the W_2 phase was observed for samples kept in freezing temperatures of −20 °C and −80 °C, with 5.10 log CFU/mL of viable bacteria observed in the W_2 phase out of the overall viable cell count of 5.19 log CFU/mL (for samples kept at −20 °C) and 4.90 log CFU/mL of viable bacteria observed in the W_2 phase out of the overall viable cell count of 4.93 log CFU/mL (for samples kept at −80 °C). Only 2.75 log CFU/mL of cells were released into the W_2 phase out of the overall viable cell count of 6.42 log CFU/mL for samples kept at 25 °C, and 2.77 log CFU/mL of cells were released out of the overall viable cell count of 6.18 log for samples kept at CFU/mL at 5 °C.

The release of bacteria from samples kept at 25 °C and 5 °C was mainly attributed to the rupture of the thin film that separates the W_1 phase from the W_2 phase, induced by the change in the osmotic balance of the droplet due to the production of bacterial by-products during the storage period. Conversely, the complete destabilisation of the

$W_1/O/W_2$ emulsion droplet stored at frozen temperatures is due to the freeze–thawing process that leads to phase separation. This process resulted in the complete release of the encapsulated bacteria as the emulsion destabilises into a layer of the bulk oil phase (top), O/W emulsion (middle), and the aqueous phase (bottom) containing the released bacteria.

As the inner W_1 phase remains intact during the freezing process (Figure 2f), the frozen $W_1/O/W_2$ emulsion may serve as an alternative for bacterial microencapsulation, whereby the controlled release of the encapsulated bacteria at the desired time can be achieved by simply thawing the frozen emulsion samples, causing immediate and complete release of the bacteria into the W_2 phase. Emulsion destabilisation induced by the freeze–thawing process has been used extensively in various applications, such as in emulsion liquid membrane (ELM) processing [62,63] and waste emulsion treatment, such as in oil sludge demulsification [33,34].

Its application in pharmaceuticals was also discussed previously by Bernal-Chávez et al. [21]. Moreover, a study by Rojas and Papadopoulos [17] also revealed the potential application of $W_1/O/W_2$ emulsion droplets for the controlled release of encapsulated materials triggered by the thawing of the oil phase. Similar to the results obtained in this study, the internal coalescence of the inner W_1 phase and the external coalescence of the outer W_2 phase were not observed during the freezing stage but occurred extensively during the thawing of the oil phase, which led to the complete release of the encapsulated material (Figure 7).

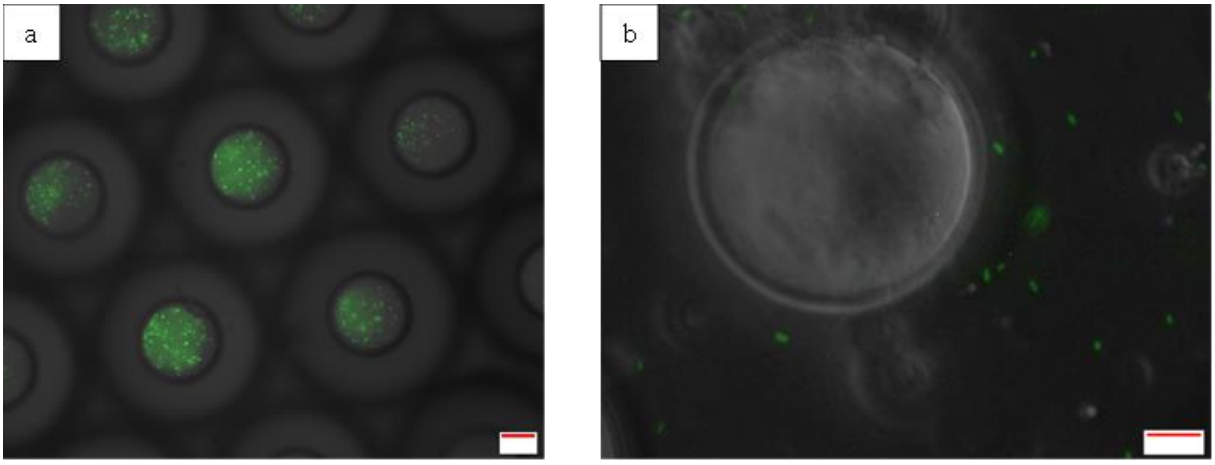

Figure 7. Photomicrographs of double-emulsion droplets before (**a**) and after (**b**) storage at −80 °C for 24 h. Scale bar represents 20 µm.

Further studies were also conducted on its potential application to the controlled release of protein from bulk emulsion systems [18]. As expected, similar results were also obtained in the bulk emulsion systems, whereby the stability of the droplet was maintained during the freezing process, while the thawing of the oil phase led to an instant release of the encapsulated protein.

4. Conclusions

This study revealed the feasibility of using emulsion droplets for bacterial encapsulation and storage not only at ambient but also at cold temperatures. The findings demonstrate that emulsion-based encapsulation enhances bacterial viability at low temperatures and that temperature changes can modulate the release of bacteria. This study provides a better understanding of the stability of emulsions in the presence of bacteria in cold temperatures and demonstrates the benefits of encapsulation in maintaining the viability of the bacteria by providing protection against the lethal effect of the freezing process.

These characteristics are beneficial for the production of emulsions containing bacteria for laboratory-based and industrial applications. In addition, it also demonstrates the poten-

tial use of the freeze–thaw technique for the controlled release of not only bacteria but also for other applications using temperature-sensitive compounds, such as in drug delivery.

Nevertheless, further studies are still required in order to compare the freeze–thaw mechanism of highly monodispersed $W_1/O/W_2$ droplets containing a single W_1 inner phase with those containing multiple W_1 inner phases, as it may exhibit a different mechanism, as observed in the absence of a second peak in the cooling curves of the double-emulsion droplet. In addition, further studies are also required to investigate the process underlying the ability of bacterial cells to maintain droplet stability during cold-temperature storage and to improve bacterial stability during the freezing process, especially for samples encapsulated in double $W_1/O/W_2$ droplets.

Supplementary Materials: The following supporting information can be downloaded at: https://www.mdpi.com/article/10.3390/fluids9120274/s1, Figure S1: Microscopic observation of emulsion destabilisation with the change in temperature; Figure S2: The bacterial adherence to soybean oil assay for live and dead *E. coli*-GFP at different soybean oil volumes.

Author Contributions: Conceptualisation, N.S.M.I.; Formal analysis, N.S.M.I.; Investigation, N.S.M.I.; Methodology, N.S.M.I., H.E.K., D.V. and K.G.; Project administration, D.V. and K.G.; Resources, D.V. and K.G.; Supervision, D.V. and K.G.; Validation, H.E.K. and D.V.; Visualisation, H.E.K. and N.F.A.M.Z.; Writing—original draft, N.S.M.I. and H.E.K.; Writing—review and editing, D.V., N.F.A.M.Z. and K.G. All authors have read and agreed to the published version of the manuscript.

Funding: This research was funded by the Ministry of Higher Education Malaysia (MOHE) as part of a doctorate programme.

Data Availability Statement: The original contributions presented in the study are included in the article and Supplementary Materials; further inquiries can be directed to the corresponding author.

Acknowledgments: The authors acknowledge the Ministry of Higher Education (MOHE), Malaysia, for funding the research as part of a doctorate programme. The authors would like to thank Iqram Fauzi, Putu Virgina Partha Devanthi, and Elaine Mitchell for their technical support. The PGPR was kindly provided by Danisco (Denmark).

Conflicts of Interest: The authors declare no conflicts of interest.

References

1. Chavarri, M.; Maranon, I.; Carmen, M. Encapsulation Technology to Protect Probiotic Bacteria. In *Probiotics*; Rigobelo, E.C., Ed.; IntechOpen: London, UK, 2012; pp. 502–529.
2. Devanthi, P.V.P.; Linforth, R.; El Kadri, H.; Gkatzionis, K. Water-in-oil-in-water double emulsion for the delivery of starter cultures in reduced-salt moromi fermentation of soy sauce. *Food Chem.* **2018**, *257*, 243–251. [CrossRef] [PubMed]
3. Peng, Q.; Meng, Z.; Luo, Z.; Duan, H.; Ramaswamy, H.S.; Wang, C. Effect of Emulsion Particle Size on the Encapsulation Behavior and Oxidative Stability of Spray Microencapsulated Sweet Orange Oil (*Citrus aurantium* var. *dulcis*). *Foods* **2023**, *12*, 116. [CrossRef] [PubMed]
4. Sobti, B.; Kamal-Eldin, A.; Rasul, S.; Alnuaimi, M.S.K.; Alnuaimi, K.J.J.; Alhassani, A.A.K.; Almheiri, M.M.A.; Nazir, A. Encapsulation Properties of *Mentha piperita* Leaf Extracts Prepared Using an Ultrasound-Assisted Double Emulsion Method. *Foods* **2023**, *12*, 1838. [CrossRef] [PubMed]
5. Dluska, E.; Markowska-Radomska, A.; Metera, A.; Tomaszewski, W. Drug-Core Double Emulsions for Co-Release of Active Ingredients. *Int. J. Chem. Eng. Appl.* **2017**, *7*, 428–432. [CrossRef]
6. Fonseca, F.; Béal, C.; Corrieu, G. Operating conditions that affect the resistance of lactic acid bacteria to freezing and frozen storage. *Cryobiology* **2002**, *43*, 189–198. [CrossRef]
7. Wang, G.; Yu, X.; Lu, Z.; Yang, Y.; Xia, Y.; Lai, P.F.-H.; Ai, L. Optimal combination of multiple cryoprotectants and freezing-thawing conditions for high lactobacilli survival rate during freezing and frozen storage. *LWT* **2019**, *99*, 217–223. [CrossRef]
8. Goderska, K.; Czarnecki, Z. Influence of microencapsulation and spray drying on the viability of Lactobacillus and Bifidobacterium strains. *Pol. J. Microbiol.* **2008**, *57*, 135–140.
9. Dianawati, D.; Mishra, V.; Shah, N.P. Survival of *Bifidobacterium longum* 1941 microencapsulated with proteins and sugars after freezing and freeze-drying. *Food Res. Int.* **2013**, *51*, 503–509. [CrossRef]
10. Nurliyani Suranindyah, Y.; Pretiwi, P. Quality and Emulsion Stability of Milk from Ettawah Crossed Bred Goat During Frozen Storage. *Procedia Food Sci.* **2015**, *3*, 142–149. [CrossRef]

11. de Farias, T.G.S.; Ladislau, H.F.L.; Stamford, T.C.M.; Medeiros, J.A.C.; Soares, B.L.M.; Arnaud, T.M.S.; Stamford, T.L.M. Viabilities of *Lactobacillus rhamnosus* ASCC 290 and *Lactobacillus casei* ATCC 334 (in free form or encapsulated with calcium alginate-chitosan) in yellow mombin ice cream. *LWT* **2019**, *100*, 391–396. [CrossRef]
12. Vanapalli, S.A.; Palanuwech, J.; Coupland, J.N. Stability of emulsions to dispersed phase crystallization: Effect of oil type, dispersed phase volume fraction, and cooling rate. *Colloids Surf. A Physicochem. Eng. Asp.* **2002**, *204*, 227–237. [CrossRef]
13. Cramp, G.L.; Docking, A.M.; Ghosh, S.; Coupland, J.N. On the stability of oil-in-water emulsions to freezing. *Food Hydrocoll.* **2004**, *18*, 899–905. [CrossRef]
14. Ghosh, S.; Coupland, J.N. Factors affecting the freeze-thaw stability of emulsions. *Food Hydrocoll.* **2008**, *22*, 105–111. [CrossRef]
15. Tippetts, M.; Martini, S. Effect of cooling rate on lipid crystallization in oil-in-water emulsions. *Food Res. Int.* **2009**, *42*, 847–855. [CrossRef]
16. Lin, C.; He, G.; Li, X.; Peng, L.; Dong, C.; Gu, S.; Xiao, G. Freeze/thaw induced demulsification of water-in-oil emulsions with loosely packed droplet. *Sep. Purif. Technol.* **2007**, *56*, 175–183. [CrossRef]
17. Rojas, E.C.; Papadopoulos, K.D. Induction of instability in water-in-oil-in-water double emulsions by freeze-thaw cycling. *Langmuir* **2007**, *23*, 6911–6917. [CrossRef]
18. Rojas, E.C.; Staton, J.A.; John, V.T.; Papadopoulos, K.D. Temperature-induced protein release from water-in-oil-in-water double emulsions. *Langmuir* **2008**, *24*, 7154–7160. [CrossRef]
19. Zhang, L.; Hu, Y.; Jiang, L.; Huang, H. Microbial Encapsulation and Targeted Delivery Mechanisms of Double Emulsion Loaded with Probiotics—A State-of-Art Review. *Food Rev. Int.* **2023**, *40*, 1731–1755. [CrossRef]
20. Guan, X.; Li, Y.; Jiang, H.; Tse, Y.L.S.; Ngai, T. Temperature-responsive Pickering double emulsions stabilized by binary microgels. *Chem.—Asian J.* **2023**, *18*, e202300587. [CrossRef]
21. Bernal-Chávez, S.A.; Romero-Montero, A.; Hernández-Parra, H.; Peña-Corona, S.I.; Del Prado-Audelo, M.L.; Alcalá-Alcalá, S.; Cortés, H.; Kiyekbayeva, L.; Sharifi-Rad, J.; Leyva-Gómez, G. Enhancing chemical and physical stability of pharmaceuticals using freeze-thaw method: Challenges and opportunities for process optimization through quality by design approach. *J. Biol. Eng.* **2023**, *17*, 35. [CrossRef]
22. Kim, P.; Kwon, K.W.; Park, M.C.; Lee, S.H.; Kim, S.M.; Suh, K.Y. Soft lithography for microfluidics: A review. *Biochip. J.* **2008**, *2*, 1–11.
23. Bauer, W.A.C.; Fischlechner, M.; Abell, C.; Huck, W.T.S. Hydrophilic PDMS Microchannels for High-Throughput Formation of Oil-in-Water Microdroplets and Water-in-Oil-in-Water Double Emulsions. *Lab Chip* **2010**, *10*, 1814–1819. [CrossRef] [PubMed]
24. Miles, B.Y.A.A.; Misra, S.S.; Irwin, J.O. The Estimation of The Bactericidal Power of The Blood. *Epidemiol. Infect.* **1938**, *38*, 732–749. [CrossRef] [PubMed]
25. Find Circles Using Circular Hough Transform—MATLAB Imfindcircles. Available online: https://www.mathworks.com/help/images/ref/imfindcircles.html (accessed on 8 October 2020).
26. El Kadri, H.; Overton, T.; Bakalis, S.; Gkatzionis, K. Understanding and Controlling the Release Mechanism of Escherichia Coli in Double W 1 /O/W 2 Emulsion Globules in the Presence of NaCl in the W 2 Phase. *RSC Adv.* **2015**, *5*, 105098–105110. [CrossRef]
27. Tieko Nassu, R.; Gonçalves, L.A.G. Determination of Melting Point of Vegetable Oils and Fats by Differential Scanning Calorimetry (DSC) Technique. *Grasas y Aceites* **1999**, *50*, 16–21. [CrossRef]
28. Harada, T.; Yokomizo, K. Demulsification of Oil-in-Water Emulsion under Freezing Conditions: Effect of Crystal Structure Modifier. *J. Am. Oil Chem. Soc.* **2000**, *77*, 859–864. [CrossRef]
29. Mezzenga, R.; Folmer, B.M.; Hughes, E. Design of Double Emulsions by Osmotic Pressure Tailoring. *Langmuir* **2004**, *20*, 3574–3582. [CrossRef]
30. Ishibashi, C.; Hondoh, H.; Ueno, S. Influence of Morphology and Polymorphic Transformation of Fat Crystals on the Freeze-Thaw Stability of Mayonnaise-Type Oil-in-Water Emulsions. *Food Res. Int.* **2016**, *89*, 604–613. [CrossRef]
31. Aronson, M.P.; Petko, M.F. Highly Concentrated Water-in-Oil Emulsions: Influence of Electrolyte on Their Properties and Stability. *J. Colloid Interface Sci.* **1993**, *159*, 134–149. [CrossRef]
32. Aronson, M.P.; Ananthapadmanabhan, K.; Petko, M.F.; Palatini, D.J. Origins of Freeze-Thaw Instability in Concentrated Water-in-Oil Emulsions. *Colloids Surf. A Physicochem. Eng. Asp.* **1994**, *85*, 199–210. [CrossRef]
33. He, G.; Chen, G. Lubricating Oil Sludge and Its Demulsification. *Dry. Technol.* **2002**, *20*, 1009–1018. [CrossRef]
34. Chen, G.; He, G. Separation of Water and Oil from Water-in-Oil Emulsion by Freeze/Thaw Method. *Sep. Purif. Technol.* **2003**, *31*, 83–89. [CrossRef]
35. Ghosh, S.; Rousseau, D. Freeze-Thaw Stability of Water-in-Oil Emulsions. *J. Colloid Interface Sci.* **2009**, *339*, 91–102. [CrossRef]
36. van Boekel, M.A.J.S.; Walstra, P. Stability of Oil-in-Water Emulsions with Crystals in the Disperse Phase. *Colloids Surf.* **1981**, *3*, 109–118. [CrossRef]
37. Degner, B.M.; Olson, K.M.; Rose, D.; Schlegel, V.; Hutkins, R.; McClements, D.J. Influence of Freezing Rate Variation on the Microstructure and Physicochemical Properties of Food Emulsions. *J. Food Eng.* **2013**, *119*, 244–253. [CrossRef]
38. Degner, B.M.; Chung, C.; Schlegel, V.; Hutkins, R.; Mcclements, D.J. Factors Influencing the Freeze-Thaw Stability of Emulsion-Based Foods. *Compr. Rev. Food Sci. Food Saf.* **2014**, *13*, 98–113. [CrossRef]
39. Mohd Isa, N.S.; El Kadri, H.; Vigolo, D.; Gkatzionis, K. Optimisation of Bacterial Release from a Stable Microfluidic-Generated Water-in-Oil-in-Water Emulsion. *RSC Adv.* **2021**, *11*, 7738–7749. [CrossRef]

40. Magdassi, S.; Garti, N. Formation of Water/Oil/Water Multiple Emulsions with Solid Oil Phase. *J. Colloid Interface Sci.* **1987**, *120*, 537–539. [CrossRef]
41. Hou, W.; Papadopoulos, K.D. Stability of Water-in-Oil-in-Water Type Globules. *Chem. Eng. Sci.* **1996**, *51*, 5043–5051. [CrossRef]
42. Zhu, X.F.; Zhang, N.; Lin, W.F.; Tang, C.H. Freeze-Thaw Stability of Pickering Emulsions Stabilized by Soy and Whey Protein Particles. *Food Hydrocoll.* **2017**, *69*, 173–184. [CrossRef]
43. Chen, Z.A.; Huang, F.; Tsai, P.A.; Komrakova, A. Numerical Study of Microfluidic Emulsion Dynamics under the Influence of Heterogeneous Surface Wettability. *Int. J. Multiph. Flow* **2022**, *147*. [CrossRef]
44. Malakshah, V.M.; Darabi, M.; Sattari, A.; Hanafizadeh, P. Numerical Investigation of Double Emulsion Formation in Non-Newtonian Fluids Using Double Co-Flow Geometry. *Chem. Eng. Res. Des.* **2024**, *203*, 165–177. [CrossRef]
45. Boode, K.; Walstra, P.; de Groot-Mostert, A.E.A. Partial Coalescence in Oil-in-Water Emulsions 2. Influence of the Properties of the Fat. *Colloids Surf. A Physicochem. Eng. Asp.* **1993**, *81*, 139–151. [CrossRef]
46. Marefati, A.; Rayner, M.; Timgren, A.; Dejmek, P.; Sjöö, M. Freezing and Freeze-Drying of Pickering Emulsions Stabilized by Starch Granules. *Colloids Surf. A Physicochem. Eng. Asp.* **2013**, *436*, 512–520. [CrossRef]
47. Souzu, H. Studies on the Damage to Escherichia Coli Cell Membrane Caused by Different Rates of Freeze-Thawing. *BBA Biomembr.* **1980**, *603*, 13–26. [CrossRef]
48. Mohd Isa, N.S.; El Kadri, H.; Vigolo, D.; Gkatzionis, K. The Effect of Bacteria on the Stability of Microfluidic-Generated Water-in-Oil Droplet. *Micromachines* **2022**, *13*, 2067. [CrossRef]
49. Firoozmand, H.; Rousseau, D. Microbial Cells as Colloidal Particles: Pickering Oil-in-Water Emulsions Stabilized by Bacteria and Yeast. *FRIN* **2016**, *81*, 66–73. [CrossRef]
50. Clausse, D.; Gomez, F.; Pezron, I.; Komunjer, L.; Dalmazzone, C. Morphology Characterization of Emulsions by Differential Scanning Calorimetry. *Adv. Colloid. Interface Sci.* **2005**, *117*, 59–74. [CrossRef]
51. Kovács, A.; Csóka, I.; Kónya, M.; Csányi, E.; Fehér, A.; Er\Hos, I. Structural Analysis of w/o/w Multiple Emulsions by Means of DSC. *J. Therm. Anal. Calorim.* **2005**, *82*, 491–497. [CrossRef]
52. Schuch, A.; Köhler, K.; Schuchmann, H.P. Differential Scanning Calorimetry (DSC) in Multiple W/O/W Emulsions: A Method to Characterize the Stability of Inner Droplets. *J. Therm. Anal. Calorim.* **2013**, *111*, 1881–1890. [CrossRef]
53. Souzu, H. Changes in Chemical Structure and Function in Escherichia Coli Cell Membranes Caused by Freeze-Thawing. I. Change of Lipid State in Bilayer Vesicles and in the Original Membrane Fragments Depending on Rate of Freezing. *BBA Biomembr.* **1989**, *978*, 105–111. [CrossRef] [PubMed]
54. Souzu, H.; Sato, M.; Kojima, T. Changes in Chemical Structure and Function in Escherichia Coli Cell Membranes Caused by Freeze-Thawing. II. Membrane Lipid State and Response of Cells to Dehydration. *BBA Biomembr.* **1989**, *978*, 112–118. [CrossRef] [PubMed]
55. Strocchi, M.; Ferrer, M.; Timmis, K.N.; Golyshin, P.N. Low Temperature-Induced Systems Failure in Escherichia Coli: Insights from Rescue by Cold-Adapted Chaperones. *Proteomics* **2006**, *6*, 193–206. [CrossRef] [PubMed]
56. Simonin, H.; Bergaoui, I.M.; Perrier-Cornet, J.M.; Gervais, P. Cryopreservation of Escherichia Coli K12TG1: Protection from the Damaging Effects of Supercooling by Freezing. *Cryobiology* **2015**, *70*, 115–121. [CrossRef] [PubMed]
57. O'Brien, K.V.; Aryana, K.J.; Prinyawiwatkul, W.; Ordonez, K.M.C.; Boeneke, C.A. Short Communication: The Effects of Frozen Storage on the Survival of Probiotic Microorganisms Found in Traditionally and Commercially Manufactured Kefir. *J. Dairy Sci.* **2016**, *99*, 7043–7048. [CrossRef]
58. Powell-Palm, M.J.; Preciado, J.; Lyu, C.; Rubinsky, B. Escherichia Coli Viability in an Isochoric System at Subfreezing Temperatures. *Cryobiology* **2018**, *85*, 17–24. [CrossRef]
59. Mazur, P. Freezing of Living Cells: Mechanisms and Implications. *Am. J. Physiol.-Cell Physiol.* **2017**, *247*, C125–C142. [CrossRef]
60. Priya, A.J.; Vijayalakshmi, S.P.; Raichur, A.M. Enhanced Survival of Probiotic Lactobacillus Acidophilus by Encapsulation with Nanostructured Polyelectrolyte Layers through Layer-by-Layer Approach. *J. Agric. Food Chem.* **2011**, *59*, 11838–11845. [CrossRef]
61. Sánchez, A.; Contreras, A.; Jiménez, J.; Luengo, C.; Corrales, J.C.; Fernández, C. Effect of Freezing Goat Milk Samples on Recovery of Intramammary Bacterial Pathogens. *Vet. Microbiol.* **2003**, *94*, 71–77. [CrossRef]
62. Hirai, T.; Hodono, M.; Komasawa, I. Preparation of Spherical Calcium Phosphate Fine Particles Using an Emulsion Liquid Membrane System. *Langmuir* **2000**, *16*, 955–960. [CrossRef]
63. Hirai, T.; Hariguchi, S.; Komasawa, I.; Davey, R.J. Biomimetic Synthesis of Calcium Carbonate Particles in a Pseudovesicular Double Emulsion. *Langmuir* **2002**, *13*, 6650–6653. [CrossRef]